https://doi.org/10.5194/egusphere-2026-2298
Preprint. Discussion started: 6 May 2026
© Author(s) 2026. CC BY 4.0 License.

Investigating the transition in ice-dynamics from a land- to lake-terminating glacier using a simple glacier dynamics model

Jaime Otero[1,2], Daniel Goldberg[1], Peter Nienow[1], Yefan Wang[1]

[1]School of Geosciences, University of Edinburgh, Edinburgh, UK
[2]ETSI de Telecomunicación, Universidad Politécnica de Madrid, Spain

Correspondence to: Jaime Otero (joterog@ed.ac.uk)

Abstract.

Glaciers interact with adjacent proglacial lakes through a range of thermomechanical processes. These interactions occur in addition to climate-driven ablation and are capable of amplifying or modifying climatic effects through various feedback mechanisms. In particular, the connection between lake water-level and the subglacial hydrological system can reduce basal friction, which in turn leads to increased glacier flow and dynamic thinning. This creates a positive feedback loop in which decreased effective pressure, also driven potentially by negative surface mass balance, enhances flow velocity, in line with similar processes observed at marine-terminating glaciers.

Our aim in this study is to develop a simple model that can be used to understand the critical controls on the dynamic behaviour of glaciers as they transition from land- to lake-terminating systems. Here, we investigate the behaviour of Skaftafellsjökull in Iceland, which has undergone such a transition over the past twenty-five years. More specifically, we use the Shallow Shelf Approximation (SSA) in Elmer Ice to model ice dynamics, incorporating a water pressure-dependant friction law to model basal sliding with a simple parameterization of basal water pressure.

The model successfully reproduces the observed velocity patterns, capturing the shift from downstream deceleration near the front in 2010 to slight acceleration in 2018, reflecting the growing influence of the proglacial lake. We find a threshold behaviour between basal water pressure and ice velocity, whereby small increases in water pressure beyond a critical value led to strong acceleration, consistent with previous empirical observations. Furthermore, our results imply that surface thinning exerts a stronger control on the near terminus acceleration than the observed terminus retreat. Our results suggest that the modelling framework developed provides a valuable tool for simulating these complex interactions in a computationally efficient manner.

1. Introduction

Lake-terminating glaciers interact with adjacent proglacial lakes through a series of thermomechanical processes (Carrivick and Tweed, 2013; Truffer and Motyka, 2016; Tsutaki et al., 2011). These processes operate in addition to climate-driven surface ablation, but these systems may also interact via multiple feedback mechanisms. Calving events can temporarily destabilize the ice margin, partially decoupling glacier dynamics from climatic forcing (Kirkbride, 1993). Furthermore, since there is a hydraulic connection between the proglacial lake and the subglacial drainage system, basal friction is reduced, facilitating higher glacier flow speeds, through a reduction in basal resistance (Carrivick et al., 2020). The resulting acceleration promotes dynamic thinning (Trüssel et al., 2013; Tsutaki et al., 2019), initiating positive feedback in which thinning decreases effective pressure which in turn enhances basal motion and further increases flow velocity (Sugiyama et al., 2011). Increased basal water pressure not only promotes sliding, but can also result in basal crevasse development and propagation, favouring calving (c.f. Van Der Veen, 1998). In addition, thermally-induced melting at the lake-ice interface can cause notches to develop at the water line, and this thermal undercutting can favour calving (Röhl, 2006).

Many examples of contrasting dynamics between land- and lake- terminating glaciers, with associated impacts on mass balance, can be found across the glaciated regions on Earth. For example, more negative mass balance at lake- compared with

https://doi.org/10.5194/egusphere-2026-2298
Preprint. Discussion started: 6 May 2026
© Author(s) 2026. CC BY 4.0 License.

land-terminating glaciers is observed in the Himalaya (King et al., 2019) where centre-line flow velocities of lake-terminating glaciers are also on average more than double those of land-terminating glaciers in the central and eastern Himalaya (Pronk et al., 2021). In Greenland, annual surface velocity at the terminus of the lake-terminating glacier Isortuarsuup Sermia increased by a factor of 2.5 during the period 2013-2021 while the near-terminus surface elevation thinned at a rate of -2.3 ± 1.1 m yr^{-1}, whereas velocity change at the nearby land-terminating Kangaasarsuup Sermia was minimal, and surface thinning rates were approximately half at comparable elevations (-1.2 ± 0.3 m yr^{-1}) (Holt et al., 2024).

Furthermore, in Iceland, pronounced differences in surface velocity, front retreat and surface elevation were found between the lake-terminating eastern arm and land-terminating central arm of Breiðamerkurjökull, a glacier draining Vatnajökull Ice Cap. Baurley et al. (2020) found the eastern arm's surface velocities increased from 1.0 ± 0.36 m day^{-1} in 1991 to 3.5 ± 0.25 m day^{-1} in 2015, while the central arm showed no discernible change in velocity over the same period. In addition, the eastern arm retreated ~3.5 km between 1982-2018, whereas the central arm retreated ~2 km over the same period (Baurley et al., 2020).

Icelandic glaciers have been experiencing mass loss since the end of the Little Ice Age (~1890). However, in recent decades, rates of mass loss have accelerated, with nearly half of the total mass loss since 1890 having occurred since 1994 (Aðalgeirsdóttir et al., 2020). While glacier mass loss has generally increased in recent decades, there is substantial interannual variability (Foresta et al., 2016). For instance, due to regional cooling in the North Atlantic, the average rate of mass loss since 2011 has been about 50% lower than between 1995-2010 (Noël et al., 2022), yet 2018–2019 marked one of the most extreme years of loss on record (−15 ± 1.6 Gt a^{-1}) (Aðalgeirsdóttir et al., 2020). Recent studies reveal that processes beyond surface melting, such as geothermal heating, volcanic activity and frontal ablation (via glacier calving), have played a significant role in shaping these recent patterns of glacier mass change (Jóhannesson et al., 2020). These non-surface driven processes are estimated to account for roughly 20% of total glacier mass loss since 1994, and at certain ice caps, particularly in southern Vatnajökull, they may contribute nearly 40% (Aðalgeirsdóttir et al., 2020).

Among these processes, frontal ablation at lake-terminating glaciers can be especially important, causing glaciers to lose mass rapidly and retreat independently of direct climatic influences (Benn et al., 2007b; Carrivick and Tweed, 2013). Although calving played only a minor role in glacier change during the early 20th century, its importance has risen since the mid-1990s. This is due primarily to outlet glaciers retreating into overdeepened bedrock troughs, thereby promoting the formation and growth of proglacial lakes (Aðalgeirsdóttir et al., 2020).

Notable examples include Svínafellsjökull, Breiðamerkurjökull, Hoffellsjökull and Skaftafellsjökull, all southerly-flowing outlets of Vatnajökull with bedrock troughs reaching between 150 and 200 m below sea level (Guðmundsson et al., 2019; Magnússon et al., 2012). These deep troughs facilitate rapid proglacial lake expansion, enhancing calving activity and thus accelerating terminus retreat and mass loss (Dell et al., 2019; Hannesdóttir et al., 2015). Such trends are expected to persist into the future, not only in Iceland but globally given trends in increasing proglacial lake extent (Zhang et al., 2024b), with major implications for glacier dynamics and regional hydrology (Schomacker, 2010). As a result, there is a pressing need to improve our ability to model the current and future dynamics of glaciers terminating in these evolving proglacial lake systems.

There have been several recent efforts to model lake-terminating glaciers and to compare them with land-terminating glacier systems. Sutherland et al. (2020) used the vertically integrated ice flow model, BISICLES, to analyse the effects of a potential proglacial lake on the retreat of the Pukaki Glacier, New Zealand, since the Last Glacial Maximum. The proglacial lake produced a maximum effect of a four-fold increase in grounding line recession and an eight-fold increase in ice velocities, relative to simulations of a land-terminating glacier forced by the same climate. Elsewhere, a depth integrated synthetic flow line model, that implicitly employed the Shallow Shelf Approximation (SSA), and assumed that subglacial water pressure follows a piezometric surface equivalent to 60% of the ice thickness away from the ice front, suggested that changes in force balance at the glacier termini are likely to play a key role in accelerating near-terminus glacier flow, with variations in basal friction being of only minimal importance (Pronk et al., 2021).

The modelling approaches used for marine-terminating glaciers also have considerable relevance and potential for investigating the dynamics of lake-terminating glaciers given the numerous similar characteristics of both systems (Benn et al., 2007b). However, certain mechanisms that concern marine-terminating glaciers are not relevant on lake-terminating glaciers; for example, submarine melting produced by buoyant freshwater plumes from subglacial discharge (Jenkins, 2011),

https://doi.org/10.5194/egusphere-2026-2298
Preprint. Discussion started: 6 May 2026
© Author(s) 2026. CC BY 4.0 License.

are absent at lake-terminating glaciers due to the lack in density contrast between the subglacial discharge and freshwater proglacial lake.

In this study, our aim is to develop a simple model that can be used to understand the critical controls on the dynamic behaviour of glaciers as they transition from land- to lake-terminating systems. More specifically, we used the Shallow Shelf Approximation (SSA), one of the simplest approximations to the full Stokes stress balance, to model glacier velocity. The model was applied to Skaftafellsjökull, a glacier in Iceland that has recently changed from land to lake-terminating. Free parameters of the model are tuned at two different times (2010 and 2018) corresponding with a period which straddles this transition, but also years when both surface velocity and surface elevation datasets are available. The near terminus glacier dynamics are subsequently projected to 2030. The aim is to investigate the changes in dynamics that occur during transition from a land- to lake-terminating glacier and the mechanisms responsible for such changes, through using a simple and computationally efficient model. Initial experiments were undertaken to determine the relationship between basal water pressure, effective pressure and ice velocities. The work then sought to determine the contrasting roles of surface thinning and ice front retreat on the force balance and thus ice motion. Finally, the work aimed to determine the overall rate of frontal (lake-terminus) ablation and the potential impact of lake-influenced ice-dynamics in amplifying glacier mass loss.

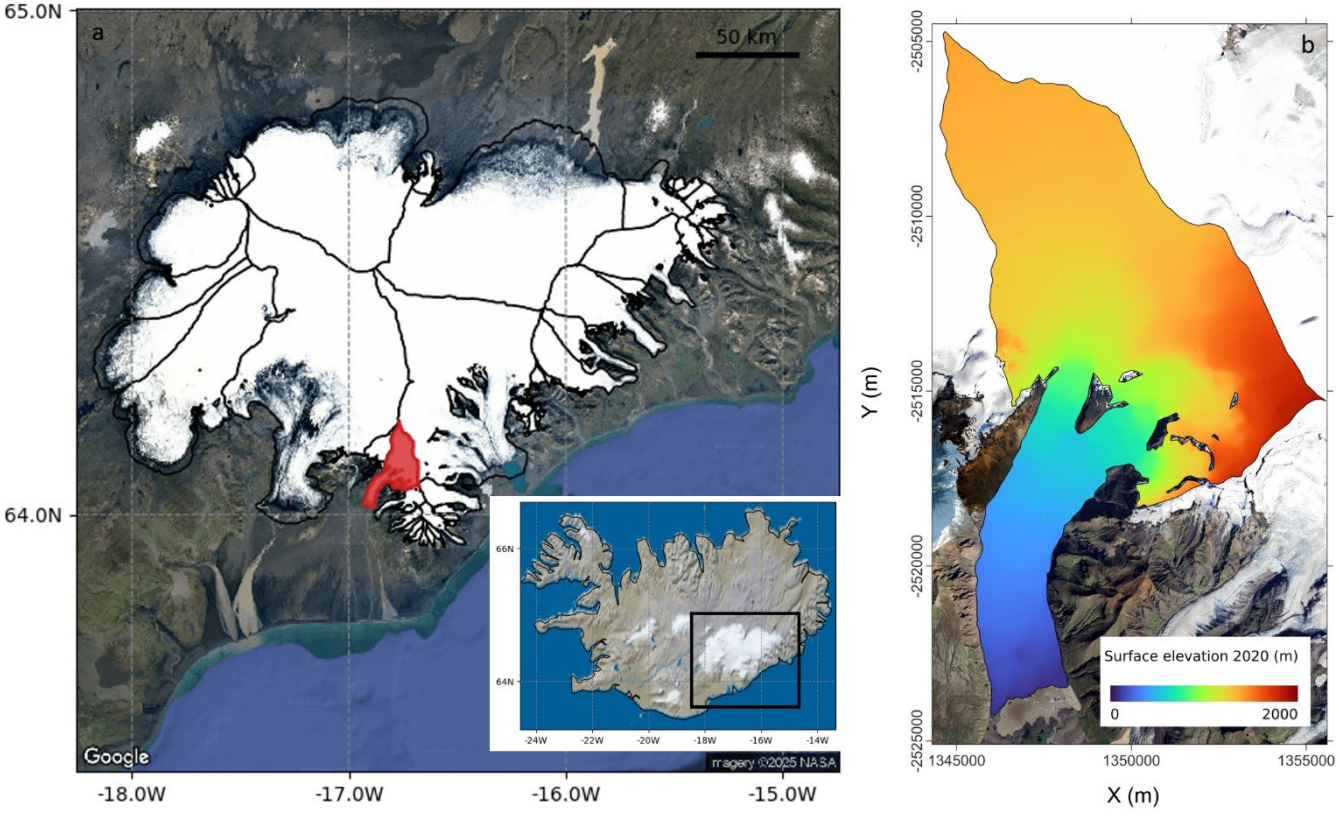


Figure 1 a) Location of Skaftafellsjökull (in red) and Vatnajökull Ice Cap with glacier outlines from the Randolph Glacier Inventory (RGI). Inset shows the location of Vatnajökull Ice Cap in Iceland. b) 2020 Surface elevation map from ArcticDEM. Background images from Google Maps (Imagery © 2026 NASA, Map data © 2026 Google).

https://doi.org/10.5194/egusphere-2026-2298
Preprint. Discussion started: 6 May 2026
© Author(s) 2026. CC BY 4.0 License.

2. Data and methods

2.1 Study site

Skaftafellsjökull is a small valley outlet glacier located on the western side of Öræfajökull Ice Cap, which itself is situated on the southern margin of Vatnajökull Ice Cap, SE Iceland (Figure 1a). Skaftafellsjökull, with an area of 84.1 km^2 in 2010 (Baurley et al., 2025), descends from 1500 m elevation on the north-western margin of Öræfajökull to ~100 m a.s.l. (Figure 1b) before terminating in an unnamed proglacial lake which starting forming around 2001. The lake had expanded to ~1.3 km^2 by 2018, with an average depth of 23 m and surface elevation at 87 m and developed initially as multiple small lakes that grew rapidly and merged into a single lake in 2011 (Guðmundsson et al., 2019). The glacier has a substantial high-altitude accumulation area which drains to a narrow ~2 km wide tongue, via an ice fall flowing between several nunataks (Figure 1b). The lower glacier tongue flows across an overdeepened bed extending up to 200 m below sea level (Figure 2).

Two key features make Skaftafellsjökull an ideal candidate for developing a model seeking to understand the critical processes operating when a glacier transitions from land- to lake-terminating. Firstly, the glacier is in the early stages of such a transition with ongoing retreat since the initial appearance of the proglacial lake in 2000, and secondly, there is a substantial volume of high resolution spatial and temporal data available, including bed geometry, surface velocity, surface elevation and terminus position during the transition period.

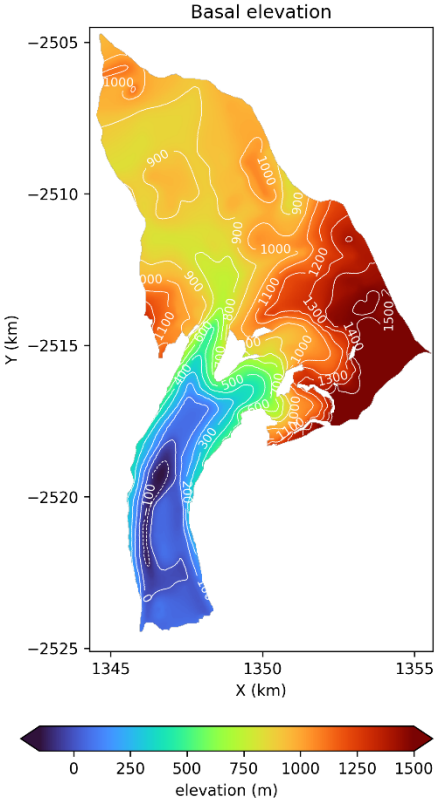


Figure 2 Bed topography of Skaftafellsjökull derived from RES surveys (Magnússon et al., 2012, 2014) **showing a substantial overdeepening extending to below sea-level (dark blue zone) in the central part of the glacier tongue.**

https://doi.org/10.5194/egusphere-2026-2298
Preprint. Discussion started: 6 May 2026
© Author(s) 2026. CC BY 4.0 License.

2.2 Data

2.2.1 Glacier terminus positions

Ice-front positions were derived by manually delineating the terminus of the glacier for each year between 1985 and 2024 using the Google Earth Engine Digitisation Tool (GEEDiT: Lea, 2018). The delineations were performed on ASTER, Landsat 5-8, and Sentinel-2 satellite imagery. To ensure consistency across the time series, termini were preferentially digitized from images acquired near the end of the melt season (i.e., August-September), capturing the glacier's minimum annual extent. Width-averaged terminus position change was subsequently quantified using the rectilinear box method (Moon and Joughin, 2008).

Skaftafellsjökull's terminus was approximately stable between 1985 and 1999 with a mean retreat rate of 3.5 m yr^{-1}. Glacier retreat then accelerated, especially across the eastern margin, at a mean rate of 50 m yr^{-1} from 2000 to 2024. Over the whole period from 1985 to 2024, the front retreated on average more than 1.2 km of which ~1.1 km was after 2000, following retreat of the terminus into the proglacial lake (Figure 3).

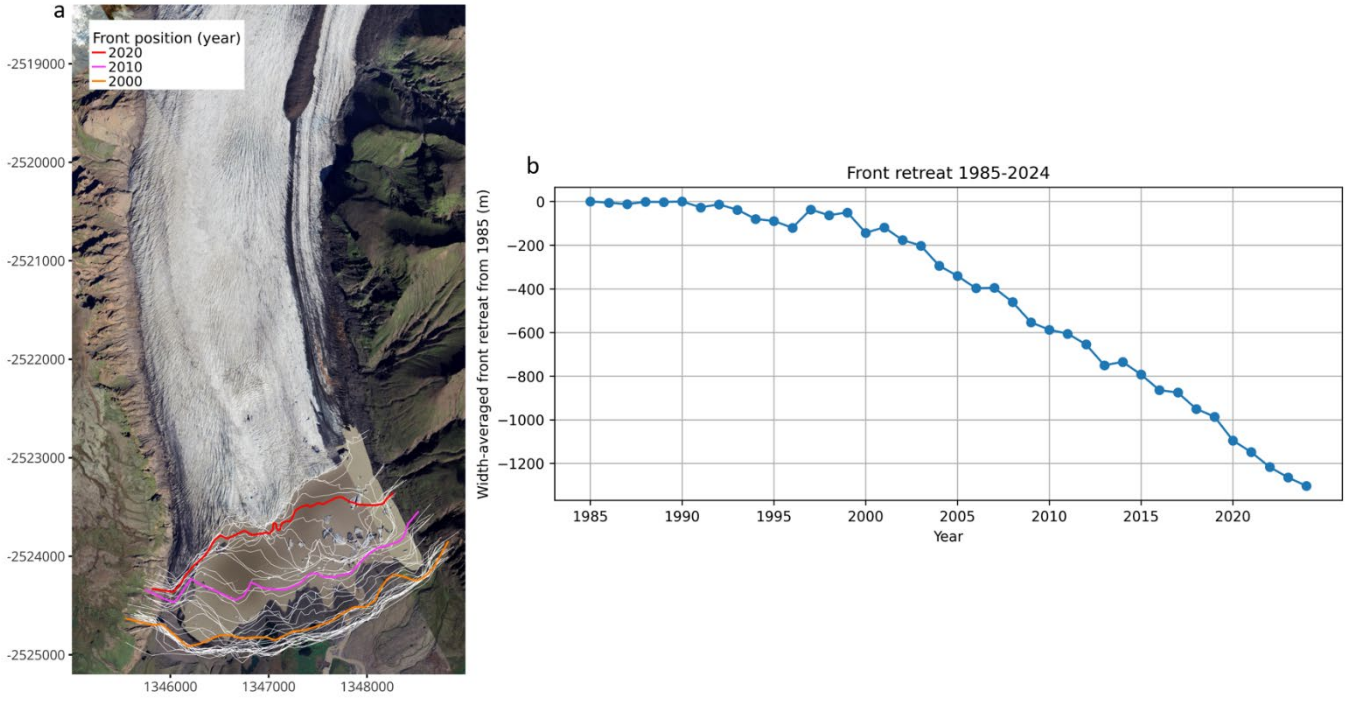


Figure 3 a) Front positions of Skaftafellsjökull between 1985 and 2024 (white lines) derived from ASTER, Landsat 5-8, and Sentinel-2 satellite imagery with positions in 2000 (orange), 2010 (pink) and 2020 (red) highlighted. Background image from Google Satellite (Imagery © 2026 Airbus, Maxar technologies, CNES / Airbus, Map data © 2026). b) Width-averaged front retreat from 1985.

2.2.2 Surface elevation

The surface DEM for 2010 was obtained from the surface DEM of Öræfajökull Ice Cap derived from airborne LiDAR surveys (Jóhannesson et al., 2013). The 2018 and 2020 ice surface elevations were derived from Arctic DEM strips, using high-resolution (0.32 to 0.5 m) Maxar satellite imagery with a spatial resolution of 2 m (Porter et al., 2022). These DEMs were co-

https://doi.org/10.5194/egusphere-2026-2298
Preprint. Discussion started: 6 May 2026
© Author(s) 2026. CC BY 4.0 License.

145 registered to the stable, ice-free terrain of the Arctic DEM Mosaic (Porter et al., 2022). The DEMs were corrected for horizontal and vertical biases using the method proposed by Nuth and Kääb (2011), implemented by the Python package xDEM (xDEM contributors, 2024).

Between 2010 and 2018, the glacier showed a slight thickening in the accumulation area (mean value of 1.1±0.45 m yr^{-1}) and a thinning across the tongue (mean value of -1.9±1.5 m yr^{-1}), which is more rapid near the glacier terminus (more than -7 m
150 yr^{-1}) (Figure 4c).

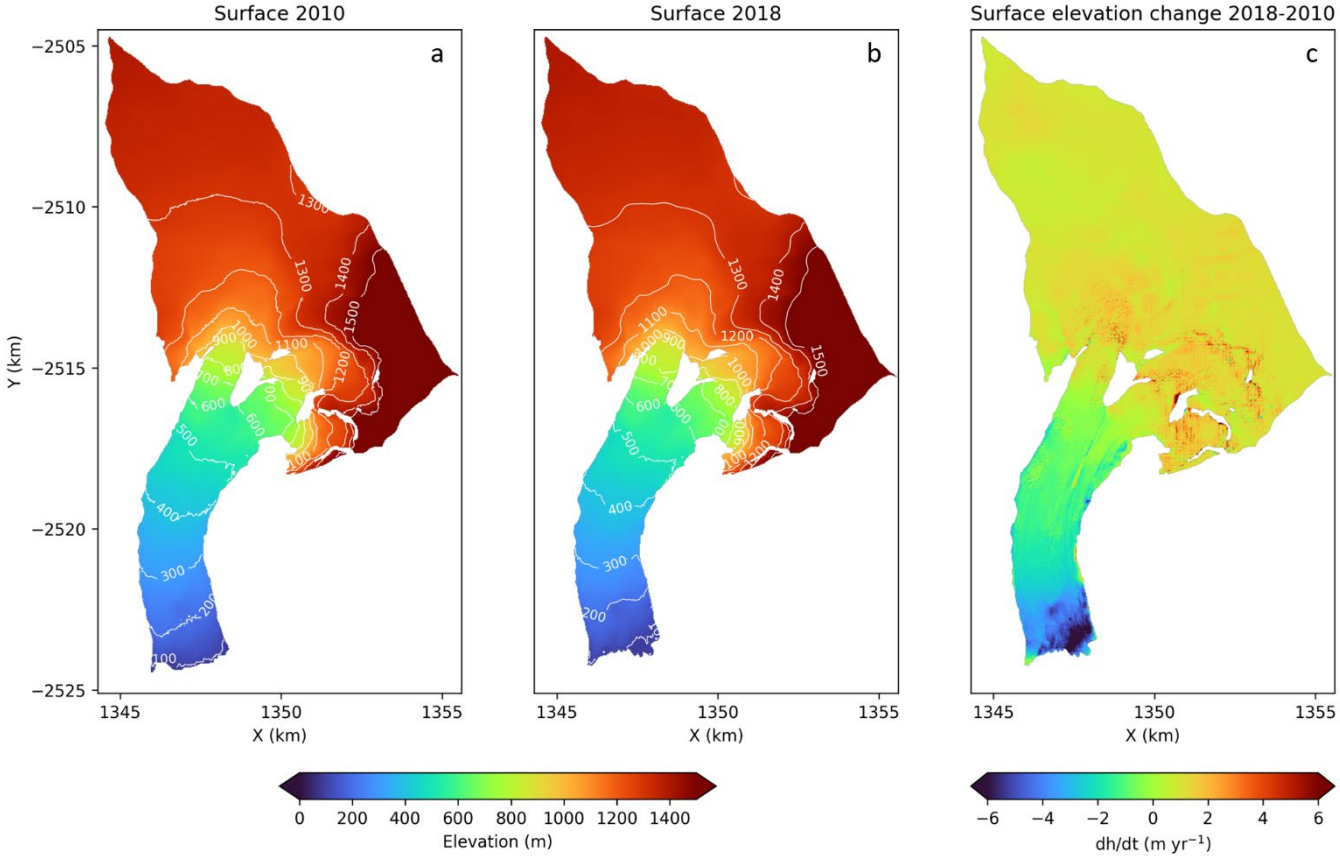


Figure 4 a) 2010 surface elevation DEM from airborne LiDAR surveys. b) 2018 surface elevation DEM from ArticDEM. c) Rate of surface elevation change (2010 – 2018) showing thinning near the glacier front.

155 ### 2.2.3 Bed elevation

The bed elevation at Skaftafellsjökull is obtained from the bedrock DEM of Öræfajökull Ice Cap, derived from radio echo sounding (RES) profiles at higher elevations on the ice cap (>1250m) and RES point measurements in the lower tongue (below ~900m elevation), and carried out between 1991 and 2012 (Magnússon et al., 2012, 2014).

The bed data derived from the RES point measurements have a higher error than areas surveyed with RES profiles because
160 firstly, migration of this type of dataset is not possible due to its discrete nature, and secondly, the data discontinuity makes misinterpretation of the bedrock reflection more likely than for the continuous RES measurements (Magnússon et al., 2012). For these reasons, the error in determining the bed at the tongue of the glacier could be substantial (and is estimated by Magnusson et al as ±20 m).

https://doi.org/10.5194/egusphere-2026-2298
Preprint. Discussion started: 6 May 2026
© Author(s) 2026. CC BY 4.0 License.

The most important feature of the glacier's basal geometry, in terms of potential proglacial lake development, is a substantial overdeepening present in the central part of the tongue. This depression reaches up to 200 m below sea level, with a maximum depth 5.2 km upglacier from the 2000 terminus, and extends from immediately downglacier of the ice fall to beyond the current glacier terminus, where the proglacial lake is now present (Figure 2 and Figure 3).

2.2.4 Surface velocities

Surface velocities were generated using the offset tracking algorithm within the European Space Agency (ESA) Sentinel Application Platform (SNAP) by Baurley et al. (2025). These velocity data were generated from imagery acquired in late summer (August-September), hence they only represent late-summer velocities, not annual averages. This study is focused on the role of lake-ice interactions on near-terminus ice-dynamics, so only surface velocities across the glacier tongue downstream of the icefall are used to compare observed and modelled velocities.

Velocities decreased down-tongue in 2010, reaching ~18 m yr^{-1} near the front (Figure 5a and Figure 7a). However, in 2018, while velocities also initially decreased down-tongue, they remained higher than in 2010 and in the terminus region, velocities actually started to increase ~1km upglacier from the terminus, reaching ~78 m yr^{-1} (Figure 5b, Figure 7b and Figure 8), near the glacier front (Baurley et al., 2025).

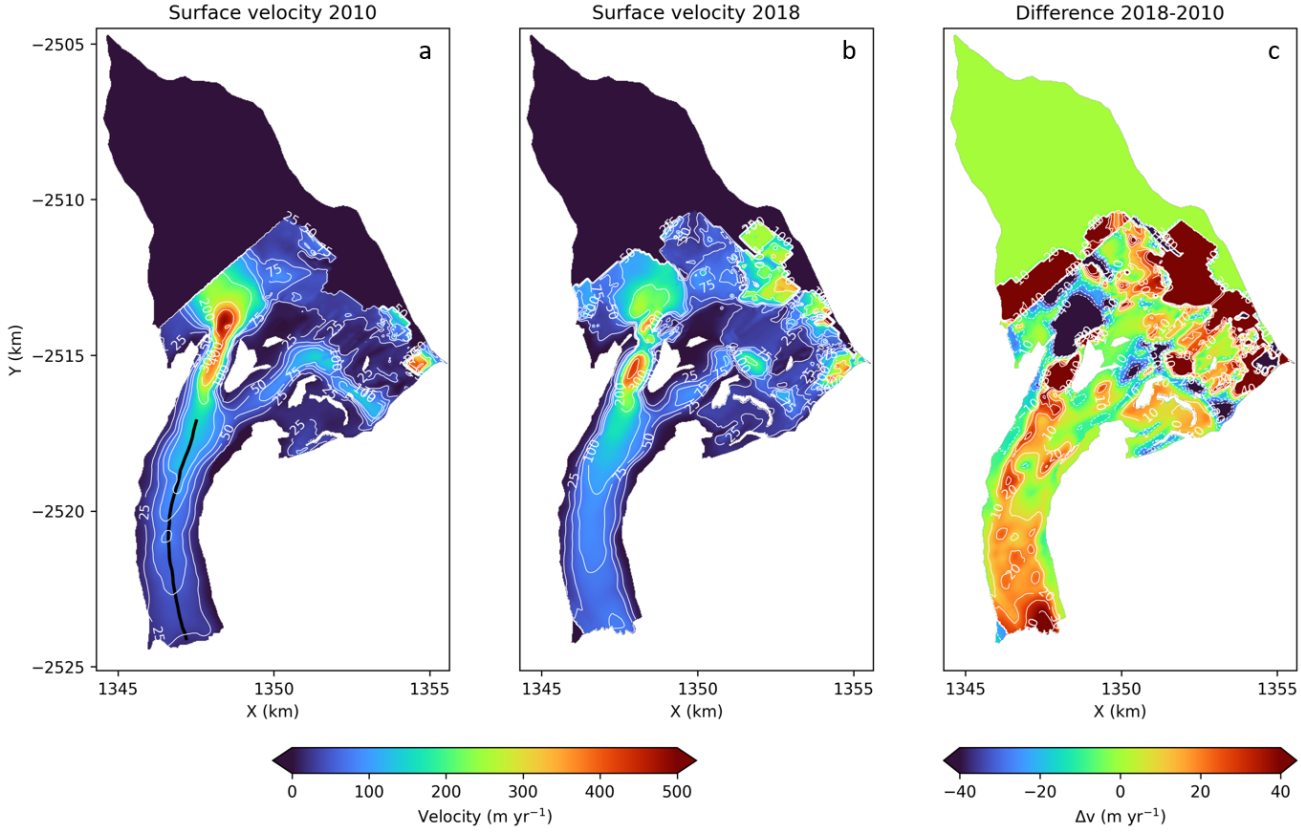


Figure 5 Maps of surface velocity derived from Sentinel (Baurley et al., 2025)**. a) 2010 surface velocity. Black line is the central flowline used in Figure 8. b) 2018 surface velocity. c) Change in velocity between 2010 and 2018.**

https://doi.org/10.5194/egusphere-2026-2298
Preprint. Discussion started: 6 May 2026
© Author(s) 2026. CC BY 4.0 License.

2.2.5 Surface mass balance

Surface mass balance (SMB) is derived from the daily output of RACMO2.3, forced by ERA reanalyses (1958–2019) statistically downscaled to a 500 m ice mask derived from the Randolph Glacier Inventory ((RGI Consortium, 2017) version 6 and the 100 m spatial resolution ArcticDEM (Porter et al., 2018), re-sampled onto a 500 m grid by Noël et al. (2022).

In the 2010-2019 period, estimated SMB for Skaftafellsjökull was positive every year except 2010 when it was slightly negative (Figure 6), concurrent with the massive eruption of Eyjafjallajökull that covered surrounding ice caps with dark volcanic tephra, reducing surface albedo (Gudmundsson et al., 2012). This period is an anomalous period of mass loss slowdown across Iceland that coincides with a regional cooling in the North Atlantic Ocean (Noël et al, 2022). Furthermore, while Icelandic glacier mass loss continued but at a slower rate during this period, Skaftafellsjökull's positive SMB reflected its unusual hypsometry with gains in the large high altitude accumulation area dominating over mass loss in the narrow ablation zone (Figure 4c).

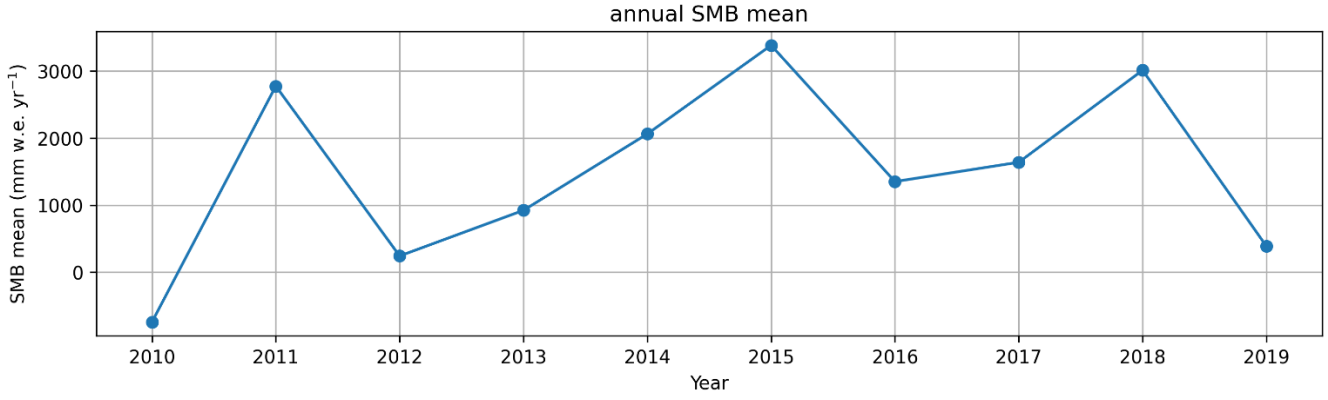


Figure 6 Annual mean of SMB of Skaftafellsjökull during the period 2010-2019 derived from RACMO.

2.3 Model

Ice models simulate the dynamic evolution of ice across multiple scales, solving ice flow equations through different approximations. One of the simplest approaches is the shallow shelf approximation (SSA; Weis et al., 1999). The SSA is suited to floating ice shelves and low-drag ice streams dominated by longitudinal (or membrane) stresses, where the driving stress is low and the ice column has an almost uniform velocity profile, i.e., plug flow (Robinson et al., 2022). The SSA model assumes a vertically constant velocity profile, such that it only accounts for the longitudinal components of the stress while neglecting the vertical components; it is then depth-integrated and thus two-dimensional (Jouvet, 2014).

As elsewhere, we infer that the glacier motion in the near-terminus region of lake-terminating Skaftafellsjökull is dominated by rapid flow due to low basal resistance, such that the deformation velocity is very small compared to sliding velocity. As a result, the approximation of generating velocities using the SSA, which only takes account of sliding, may be sufficiently accurate in the most important part of the glacier for this study, i.e., the tongue region. In this paper, all experiments are conducted using the SSA implementations of Elmer/Ice (Gagliardini et al., 2013), an open-source finite-element ice dynamic model. An unstructured finite-element mesh with triangular elements, denser near the front, is created using Gmsh (Geuzaine and Remacle, 2009) for the footprint of the glacier.

Basal water pressure plays a key role in controlling ice motion (Iken and Bindschadler, 1986) including at lake-terminating glaciers (Sugiyama et al., 2011). Here, basal sliding is parameterized using a regularized Coulomb-type friction law (Gagliardini et al., 2007; Schoof, 2005), which is a non-linear water pressure-dependent friction law, implemented in

https://doi.org/10.5194/egusphere-2026-2298
Preprint. Discussion started: 6 May 2026
© Author(s) 2026. CC BY 4.0 License.

Elmer/Ice. The dependence from the water pressure is given through the effective pressure at the ice-bed interface N, defined as the difference between ice-overburden and basal-water pressure.

Based on Gagliardini et al. (2007), the friction law can be written as

$$\tau_b = N\left[\frac{u_b}{u_b + N^n A_s}\right]^{\frac{1}{n}} \quad (1)$$

where τ_b is the basal drag, u_b is the basal velocity, n is the flow-law exponent ($n = 3$) and A_s is the sliding coefficient.

The effective pressure N can be expressed as

$$N = \rho_i g H - \rho_w g P_{wp}(z_l - z_b) \quad (2)$$

where ρ_i is the ice density, g is the acceleration due to gravity, H is the ice thickness, ρ_w is the water density, z_l is the lake surface elevation, z_b is the glacier bed elevation, and P_{wp} is a scaling parameter to take in to account the increasing water pressure above its "minimum level". This minimum level of water pressure is the pressure which corresponds with the water height equal to the elevation of the lake surface, assuming a perfect hydrological connection between the lake and the upglacier subglacial hydrological system. Assuming this mode of perfect connection between the ocean and the subglacial hydrological system is commonly used in marine-terminating glacier models (e.g., Bondzio et al., 2016; Cook et al., 2014).

P_{wp}, the water pressure parameter, is a free parameter of the model that was added to parameterize the influence of water pressure on sliding velocity through the friction law. Such a parameterization is a simplified way of representing the basal hydrology. Another way of incorporating water pressure in models would be to consider water pressure as a fraction of ice overburden pressure for bedrock below sea level, as used by Martin et al (2011) in an Antarctic Ice Sheet model, or in a model of lake terminating glaciers in the Himalaya, in which subglacial water pressure is assumed to follow a piezometric surface equivalent to a fraction of the ice thickness away from the calving front (Pronk et al., 2021).

Near the ice front, the vertical force due to the static weight of the ice exceeds the horizontal static force due to the water (Cuffey and Paterson, 2010). Therefore, a depth-integrated Neumann boundary condition was applied, following Cuffey and Paterson (2010), to model the margin stress as

$$\phi = \frac{1}{2}\rho_i g H^2 - \frac{1}{2}\rho_w g (z_l - z_b)^2). \quad (3)$$

The free parameters, water pressure parameter P_{wp}, sliding parameter A_s and viscosity parameter A were tuned running simulations with both the 2010 and 2018 geometries. For each year and geometry, 133000 simulations were run with different values of each free parameter (see Table 1a), with the aim to minimize the mismatch between the observed and modelled surface velocities in both 2010 and 2018 and also, to minimize the difference between the observed and modelled acceleration, in a region of the tongue that is 1 km wide (centred) and ~5 km long extending upglacier from the terminus; this is the so called 'tuning' region. The key aim of this tuning process is to obtain a combination of parameters where the model is able to reproduce the observed behaviour of glacier surface velocities, during the transition from land- to lake-terminating conditions. For both years, and also for the acceleration, the Mean Absolute Error (MAE) and Mean Squared Error (MSE) of velocities were calculated within the 'tuning' region.

In order to derive optimal parameters, a number of metrics were applied to the experimental ensemble, quantifying fit to various aspects of the data. The types of metrics are listed below according to the corresponding observations; note that for each type, the Mean Absolute Error (MAE) between model and observations, as well as the Mean Squared Error (MSE), is applied, unless otherwise indicated. Results and optimising parameter pairs are shown in Table 1b.

- **2010** and **2018:** the observed velocities in each year.
- **Acceleration:** the change in velocity between 2010 and 2018.
- **Mean MAE:** the algebraic mean of the **2010**, **2018**, and **Acceleration** MAEs.
- **Weighted Mean:** equivalent to $\frac{2}{3}MAE_{Acceleration} + \frac{1}{6}MAE_{2010} + \frac{1}{6}MAE_{2018}$.
- **Dist Zero:** Root mean square of the 2010, 2018 and Acceleration MAEs.
- **Mean MSE**: the algebraic mean of the **2010**, **2018**, and **Acceleration** MSEs.

https://doi.org/10.5194/egusphere-2026-2298
Preprint. Discussion started: 6 May 2026
© Author(s) 2026. CC BY 4.0 License.

Table 1 a) Minimum and maximum values of the free parameters used in the tuning process, number of values taken for each parameter (N) and best-fit set of parameters selected after the process. b) Set of free parameters found to minimize the various metrics. Bold value of each column corresponds to the minimized metric.

a)	A_S (*3.15576 MPa^{-3} a^{-1})	P_{wp}	A (MPa^{-3} a^{-1})
Minimum	10	1.1	1
Maximum	199	1.7	100
N	190	7	100
Best-fit	101	1.5	20

b)			Acceleration		2010		2018		Mean MAE	Weighted Mean	Dist zero	Mean MSE
A_s	P_{wp}	A	MSE	MAE	MSE	MAE	MSE	MAE				
101	1.5	20	43.01	4.91	59.16	5.65	48.65	5.11	**5.22**	5.07	**9.06**	50.27
100	1.5	24	42.10	4.81	58.92	5.59	53.97	5.37	5.26	**5.04**	9.12	51.66
100	1.5	19	43.47	4.96	58.90	5.73	46.43	5.11	5.27	5.11	9.14	**49.60**
101	1.5	28	42.16	**4.76**	63.93	5.70	67.42	6.10	5.52	5.14	9.60	57.83
110	1.3	14	97.99	7.68	54.55	**5.15**	114.61	8.53	7.12	7.40	12.58	89.05
107	1.5	10	49.57	5.25	67.69	6.23	39.34	**4.73**	5.40	5.33	9.42	52.20

Results show that similar sets of parameters consistently minimized the metrics tested. Therefore, the set of parameters $A_S = 101$, $P_{wp} = 1.5$ and $A = 20$ was chosen as the 'best-fit' parameters, and used subsequently for the rest of the simulations discussed in the results below.

https://doi.org/10.5194/egusphere-2026-2298
Preprint. Discussion started: 6 May 2026
© Author(s) 2026. CC BY 4.0 License.

3. Results and discussion

3.1 Surface velocity

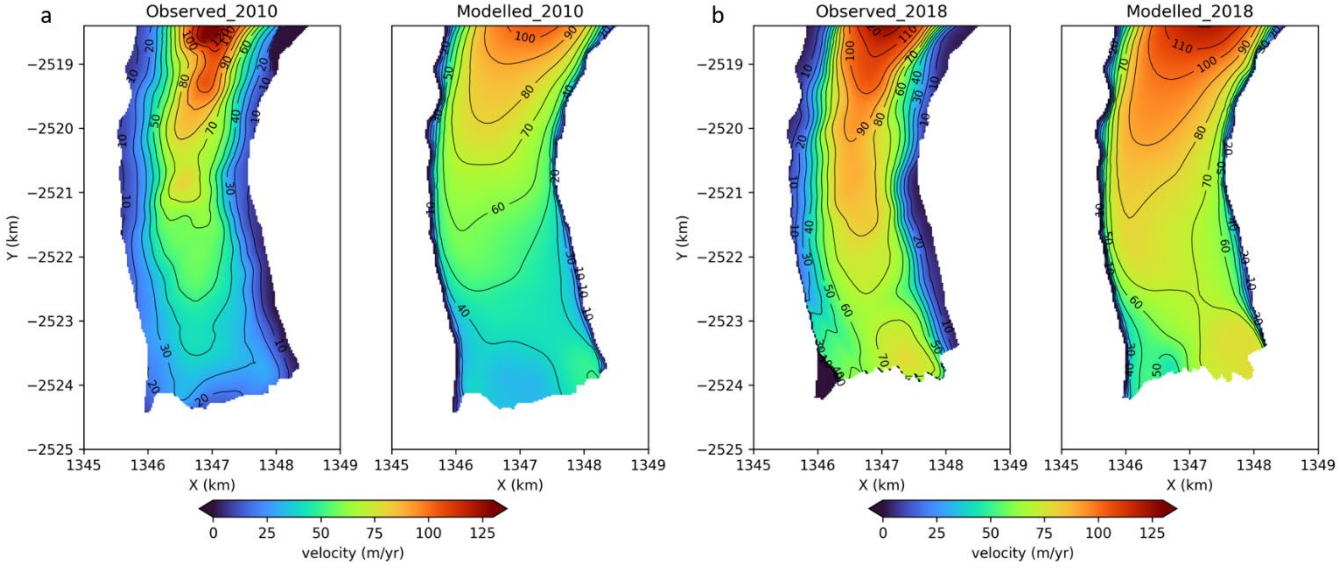


Figure 7 Detail of surface velocity maps of the glacier tongue. Velocity contours are plotted at 10 m intervals. a) Observed (left) and modelled (right) velocities for 2010 and b) observed (left) and modelled (right) velocities for 2018.

Using the 'best-fit' set of parameters found in the tuning process, the model reproduced well the surface velocities for both 2010 and 2018. The observed and modelled 2010 velocities decrease along the 5 km glacier tongue from the ice fall to the terminus, reaching minimum values of ~20 m yr^{-1} (observed) and ~30 m yr^{-1} (modelled) at the terminus (Figure 7a and Figure 8). By 2010, the glacier already terminated in the lake (Fig. 3), which is likely why the terminus velocity is nonzero, but it was shallow (~12 m maximum deep) and discontinuous across the ice front (Guðmundsson et al., 2019). As such, it seems clear that the lake was influencing glacier dynamics, but not significantly at this time. By 2018, the observed and modelled velocities also decrease initially downglacier from the ice fall, but ca. 1.5 kilometres from the terminus, both observed and modelled velocities begin to slightly increase towards the front, reaching ~78 m yr^{-1} (observed) and ~77 m yr^{-1} (modelled). This increase in near-terminus velocity, in conjunction with the pronounced terminus acceleration between 2010 and 2018, is consistent with the behaviour typical of a glacier terminating in a deepening proglacial lake (e.g., Baurley et al.,2020; Wu et al., 2025) (Figure 7b and Figure 8). By 2018, the proglacial lake extended across the full glacier terminus width, covering 1.3 km^2 and reaching ~50 m deep at its deepest point (Guðmundsson et al., 2019).

https://doi.org/10.5194/egusphere-2026-2298
Preprint. Discussion started: 6 May 2026
© Author(s) 2026. CC BY 4.0 License.

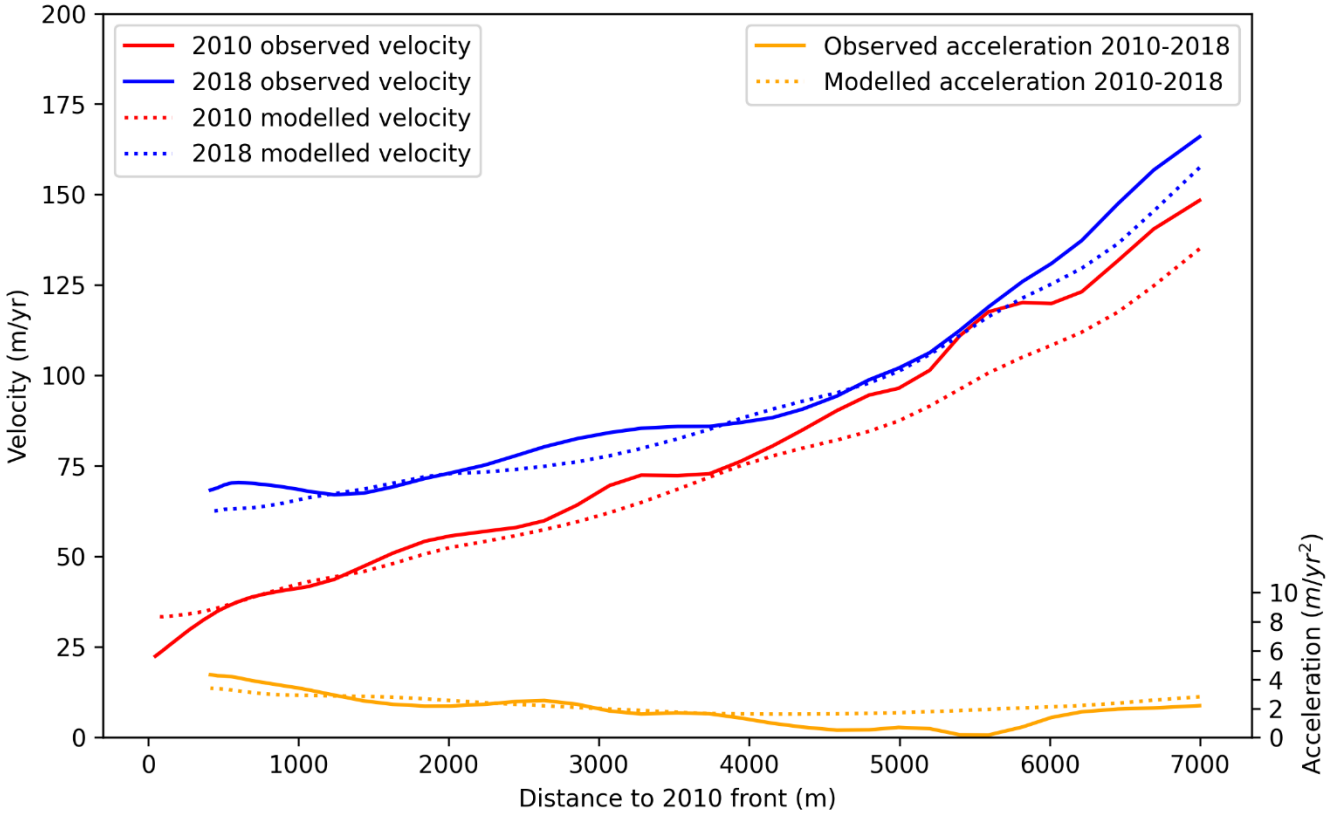


Figure 8 Comparison between observed (solid lines) and modelled (dotted lines) velocities for 2010 (red), 2018 (blue) and the 2010-2018 acceleration (orange) in a flowline along the centre of the glacier tongue (Figure 5a). Velocities at each node of the flowline, ~200 m apart, were calculated as an average of the velocities of nine points located in a 400x400 m grid centred on the node in order to avoid local effects.

In a final experimental projection, the geometry, surface elevation and front position, of the glacier was extrapolated to 2030 using the data and trends observed between 2010 and 2020, in order to predict how the glacier's dynamics might evolve over the coming decade (Figure 9a). The model was thus applied to this extrapolated geometry which projects a sustained terminus acceleration of ~12 m yr^{-2}; a higher rate than was observed between 2010-2018, resulting in near terminus velocities of up to ~265 m yr^{-1} by 2030 (Figure 9b).

https://doi.org/10.5194/egusphere-2026-2298
Preprint. Discussion started: 6 May 2026
© Author(s) 2026. CC BY 4.0 License.

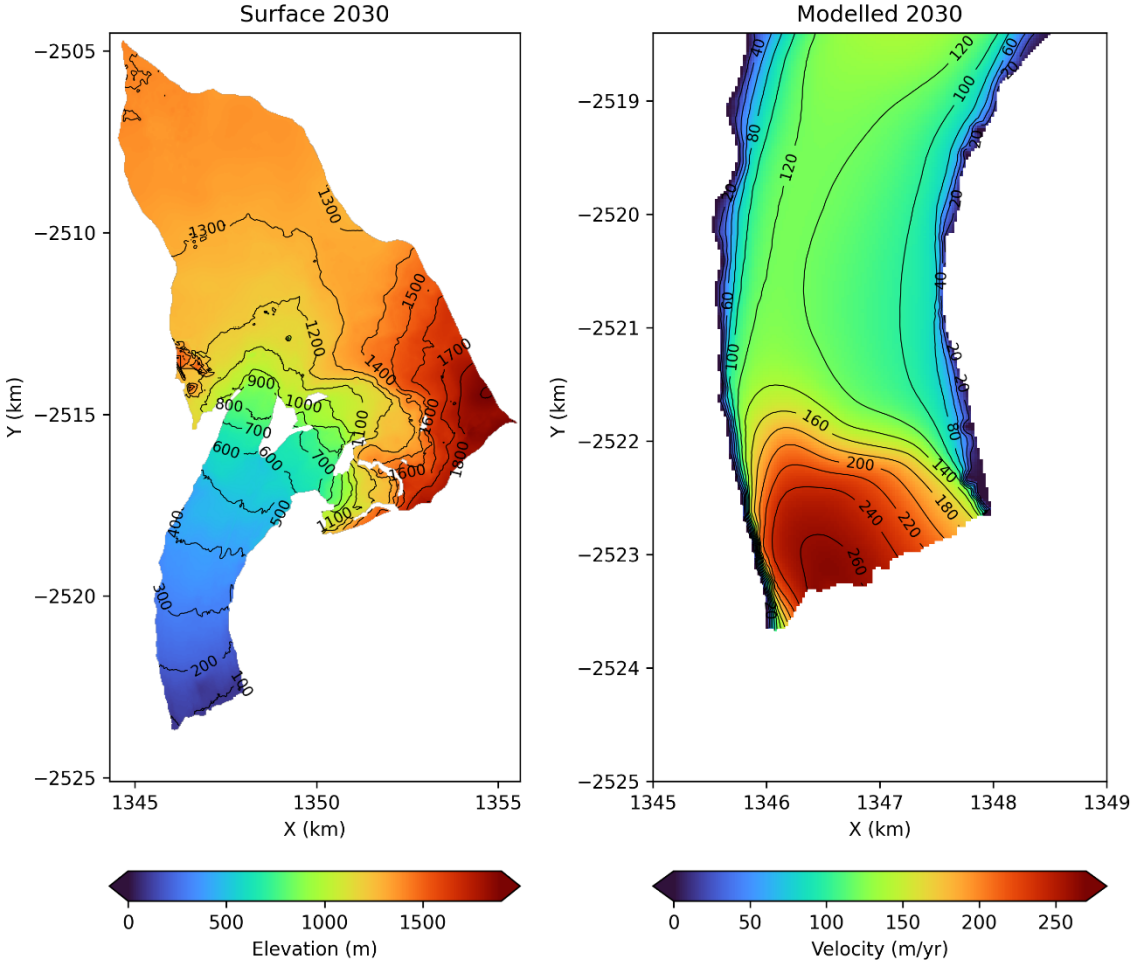


Figure 9 a) The extrapolated glacier geometry (surface elevation and front position) in 2030 b) The modelled surface velocities of the glacier tongue for based on the extrapolated 2030 geometry. Contour lines are plotted at 20 m intervals.

The increase in velocities shown by the model near the front in 2030 highlights the behaviour that this glacier may exhibit in the near future with potentially devastating consequences for glacier mass balance.

3.2 Basal water pressure

Sensitivity analyses were undertaken to evaluate the behaviour of the modelled ice velocities to different values of basal water pressure, and thus different values of effective pressure. These experiments were run for both 2010 and 2018, with the sliding parameter fixed, while varying the water pressure parameter P_{wp}, to account for different basal water pressures. We used 7 values of P_{wp}, ranging from 1.1 to 1.7 for each date, and in order to compare this parameter with a representative velocity scale, averages of the values from all of the nodes within 1.5 km of the terminus were used.

The results demonstrate that for values of water pressure less than 0.9 MPa, velocity increases linearly with water pressure with a slope of ~7 m yr^{-1} per 0.1 MPa. However, at values greater than 0.9 MPa, surface velocity scales exponentially with water pressure whereby small increments in water pressure increase velocity dramatically (Figure 10a).

https://doi.org/10.5194/egusphere-2026-2298
Preprint. Discussion started: 6 May 2026
© Author(s) 2026. CC BY 4.0 License.

These findings support previous work suggesting that there is a critical threshold in the relationship between water pressure/effective pressure, and ice velocity beyond which there is a shift from an approximately linear to a highly nonlinear relationship (Iken and Bindschadler, 1986; Sugiyama et al., 2011).

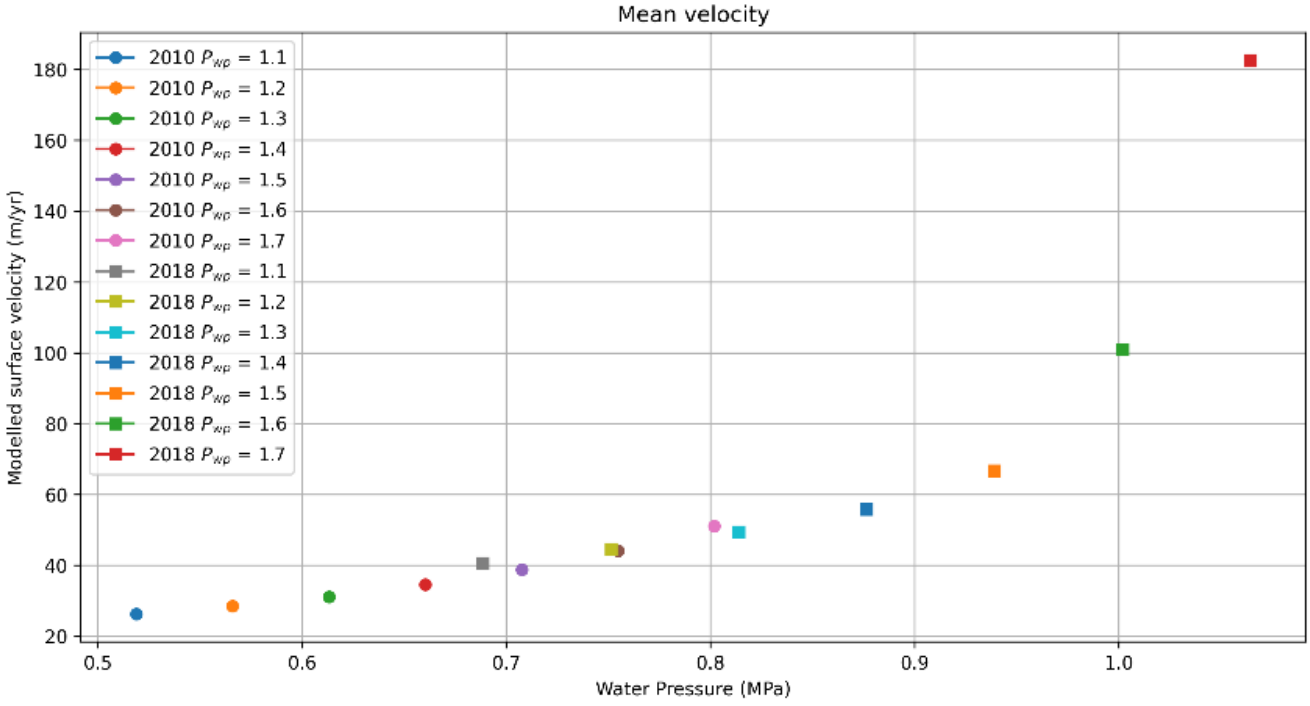


Figure 10 Mean modelled surface velocity within 1.5 km from the glacier front as a function of basal water pressure for both 2010 and 2018 and constrained by different values of the water pressure parameter P_{wp}.

3.3 Influence of front retreat and thinning on surface velocities

It is recognised that frontal ablation at tidewater glaciers can lead to acceleration due to loss of resistive stresses (i.e. backstress) in the glacier (Howat et al., 2005; Thomas, 2004). As the terminus of Skaftafellsjökull retreated from 2010 to 2020, we must consider the possibility that any changes in the observed velocity could be attributed to loss of backstress resulting from calving front retreat. In addition, sustained terminus thinning, driven by both ongoing negative surface mass balance and ice acceleration (and thus dynamic thinning) will reduce near-terminus effective pressure thereby facilitating acceleration via basal sliding (Benn et al., 2007a; Holt et al., 2024; Pfeffer, 2007). Experiments were therefore undertaken to test the competing influences of front terminus retreat and ice-thinning on surface velocities. The experiments aim to isolate the dynamic effect of frontal retreat through calving, as opposed to glacier thinning, which is driven by surface melt and dynamic thinning. The evolution with time of these competing effects was tested via two experiments, EXP1 and EXP2, over two different periods, 2010-2020 and 2020-2030. For this, five simulations were run: 1) with 2010 geometry (S10F10); 2) with 2010 surface elevation and 2020 front position (S10F20); 3) with 2020 geometry (S20F20); 4) with 2020 surface elevation and 2030 front position (S20F30); and 5) with 2030 geometry (S30F30) (see Table 2a).

Table 2 a) Simulations conducted with different geometries (surface elevation and front position) to facilitate comparative analyses between the first and second experiments. SXXFYY represents a configuration with geometry from 20XX and front position corresponding to 20YY. b) Outline of the first, EXP1, and second, EXP2, experiments for each time interval.

a)	Surface elevation	Front position

b)	Period	Experiment	Simulations involved

https://doi.org/10.5194/egusphere-2026-2298
Preprint. Discussion started: 6 May 2026
© Author(s) 2026. CC BY 4.0 License.

S10F10	2010	2010
S10F20	2010	2020
S20F20	2020	2020
S20F30	2020	2030
S30F30	2030	2030

2010-2020	EXP1	S20F20 vs. S10F20
	EXP2	S10F20 vs. S10F10
2020-2030	EXP1	S30F30 vs. S20F30
	EXP2	S20F30 vs. S20F20

The aim of the first experiment (or group of experiments) EXP1 is to isolate the effects of surface thinning on velocity. In both comparisons, front position is held constant (either in its 2020 or 2030 configuration) and surface elevation is modified (2010 vs 2020, or 2020 vs 2030, see Table 2b). The resulting velocities are then compared. Similarly, the second group, EXP2, isolates the effects of front position by holding surface constant (in either its 2010 or 2020 configuration) and modifying the front position (again, 2010 vs 2020, or 2020 vs 2030, depending on the specific experiment, see Table 2b).

These experiments, which isolate the respective effects of ice front retreat and surface thinning on ice dynamic response, demonstrate that during the first period, 2010-2020, the observed thinning exerts a far greater influence on glacier acceleration than terminus retreat, resulting in near-terminus acceleration of up to ~8 m yr^{-2}. In contrast, the front retreat, and the associated impact on buttressing and near-terminus stress-regime, produced only localized and minimal near-terminus acceleration of up to ~2 m yr^{-2}; as such, the influence of frontal retreat on ice motion was only 25% of that driven by surface thinning for the period 2010-2020 (Figure 11a). During the second period, the impact associated with front retreat becomes more important, with near-terminus acceleration of up to ~6 m yr^{-2}, while the impact of surface thinning causes acceleration of up to ~14 m yr^{-2}. The influence of front retreat therefore increases during this later period but surface thinning clearly remains the dominant driver of acceleration during the period 2020-2030 (Figure 11b). These findings suggest that changes in the stress-regime associated with thinning, rather than front retreat, play the dominant role in controlling the observed velocity evolution at Skaftafellsjökull during the transition from a land- to a lake-terminating system.

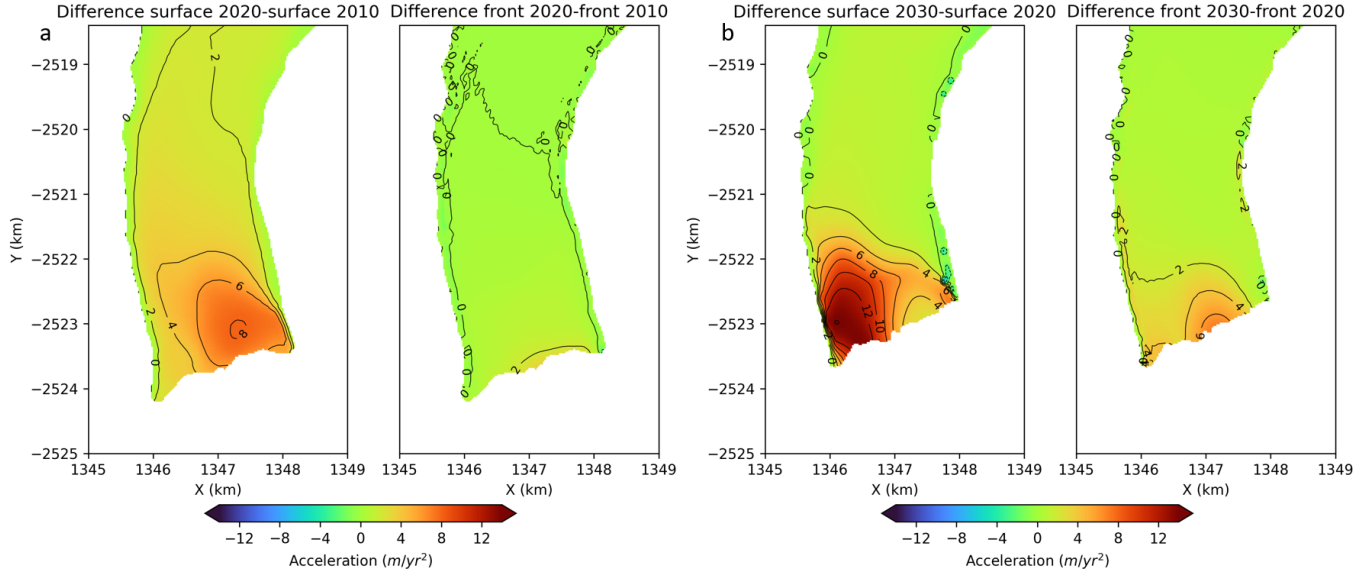


Figure 11 a) Surface acceleration of the glacier tongue for EXP1 (left) and EXP2 (right) for the 2010-2020 period. b) Detail of surface acceleration map of the glacier tongue for EXP1 (left) and EXP2 (right) for the 2020-2030 period.

https://doi.org/10.5194/egusphere-2026-2298
Preprint. Discussion started: 6 May 2026
© Author(s) 2026. CC BY 4.0 License.

3.4 Frontal ablation

Quantifying frontal ablation is of critical importance for water-terminating glaciers, either marine- or lake-terminating, in order to determine the respective proportions of mass lost by either surface melt processes or by frontal ablation, the latter which comprises both calving and subaqueous frontal melt. For example, across Greenland, recent estimates suggest that mass loss between 1992 and 2018 has come equally from both surface melt and frontal ablation at tidewater glaciers (Shepherd et al., 2020) while at Patagonian icefields, frontal ablation from 2000 to 2019 over a set of 30 lake-terminating and 15 ocean-terminating glaciers represented ~34 ± 6% of the total ablation, while for the subset of lake-terminating glaciers, frontal ablation accounted for ~25% of total ablation (Minowa et al., 2021).

Following McNabb et al. (2015), the total rate (or volume) of frontal ablation FA can be defined as the sum of the integral over the front surface of the ice velocity at the terminus u_t and the change of terminus position, FR (positive if the front is retreating). Given that the front surface is constantly changing, the integral of u_t , i.e., flux through the front, is estimated as a finite sum over a cross section (flux gate) of the glacier, located some distance upstream of the front (Figure 12b). The flux gate is divided into vertical sections with flux through each section calculated as section surface velocity u_{si}, multiplied by a factor f to take account of decreasing velocity with depth, multiplied by section area S_i, and by cosine of the angle α_i between the velocity vector and the vector normal to the flux gate surface. Finally, the flux through the flux gate is the sum of the flux through each section

$$F_{fg} = \sum_i f u_{si} S_i \cos \alpha_i \tag{4}$$

As flux gate is located some distance upstream of the front, mass changes due to surface mass balance ($\dot{b}$) after the ice passes through the fluxgate must be taken into account. The change of terminus position, FR, is calculated following the "box method" (McNabb and Hock, 2014; Moon and Joughin, 2008). Therefore, frontal ablation is defined as

$$FA = F_{fg} + FR - \dot{b} \tag{5}$$

In order to estimate changes in frontal ablation at Skaftafellsjökull through time, ice discharge through a flux gate located ~1.5 km upglacier from the 2010 terminus (Figure 12b) was calculated for each of 2010, 2018, 2020 and 2030 (Figure 12a). As the model assumes ice flow is primarily driven by sliding, we prescribe $f = 1$, and $\alpha_i = 1$ assuming the flux gate is perpendicular to the flow.

The results from the modelled estimates of ice flux show an approximately linear increase between 2010 and 2030, with a factor three increase in flux (Figure 12a), driven by the near-terminus acceleration, and despite glacier wide surface thinning (Figure 4c) which results in a reduction in the cross-sectional area at the flux gate.

https://doi.org/10.5194/egusphere-2026-2298
Preprint. Discussion started: 6 May 2026
© Author(s) 2026. CC BY 4.0 License.

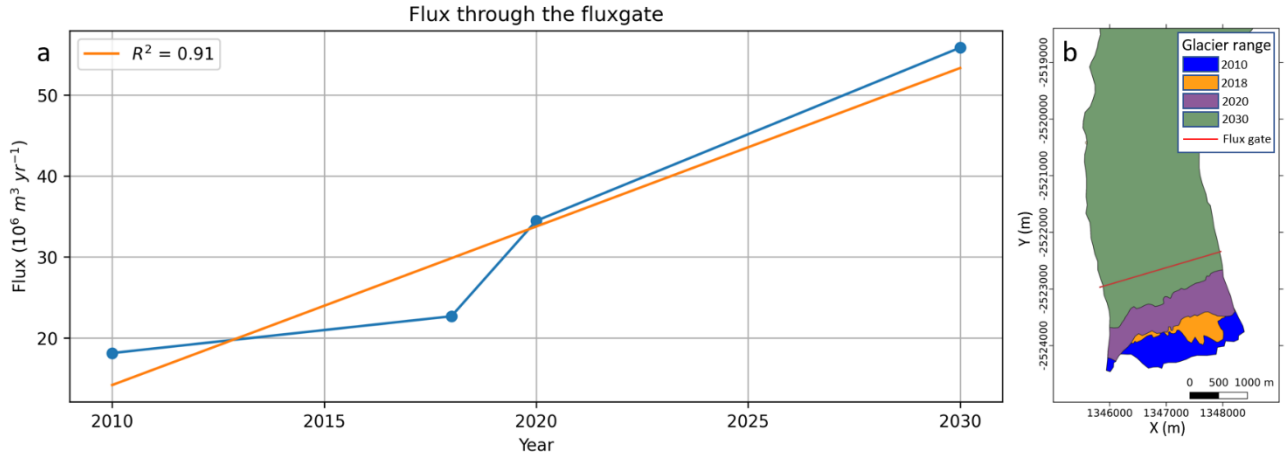


Figure 12 a) Estimates of ice flux through a flux gate, located ~1.5 km upglacier from the 2010 terminus, between 2010 and 2030. The best fit regression line (orange) reports a statistically significant increase (R^2=0.91) in flux with time. b) Location of the flux gate and the front positions for the different years.

The annual mean surface mass balance (or surface ablation $\dot{b}$) below the fluxgate for the period 2010-2018 was estimated using RACMO data, taking the cells from the RACMO grid located below the fluxgate for each year from 2010-2018, giving a mean value of mass loss of 11.8 x10^6 m^3 w.e. yr^{-1}. The mean annual frontal ablation rate between 2010 and 2018 is subsequently calculated following Equation 5. Here, the annual mean ice flux through the flux gate (18.3 x10^6 m^3 w.e. yr^{-1} (F_{fg})) between 2010 and 2018 is added to the annual mean ice-volume lost due to frontal retreat over the same period (37.2 x10^6 m^3 w.e. yr^{-1}); the annual mean surface mass balance below the fluxgate (11.8 x10^6 m^3 w.e. yr^{-1}) is then subtracted giving an annual value of frontal ablation of 43.7 x10^6 m^3 w.e. yr^{-1} (Table 3). All ice volumes are converted to water equivalent assuming a density of 900 kg m^{-3} (following Osmanoglu et al., 2014).

Annual mean surface ablation (SAbl) for the whole glacier for the period 2010-2018 was retrieved from RACMO data giving a value of 74.5 x10^6 m^3 w.e. yr^{-1}. Total mean annual ablation for the whole glacier between 2010-18 is therefore 118.2 x10^6 m^3 w.e. yr^{-1} of which frontal ablation, driven by terminus acceleration and retreat, represents ~37 % (Table 3). Frontal ablation thus emerges as a critical driver of mass loss during the study period emphasizing the growing importance of the evolving lake-induced dynamic processes, relative to surface mass balance, in governing the glacier's mass budget.

Table 3 Estimates of the different annual mean flux and ablation terms for the period 2010-2018 including, in bold, annual mean frontal ablation and total ablation.

	Annual mean (10^6 m^3 yr^{-1} w.e.)
Flux through the flux gate (F_{fg})	18.3
Surface ablation below the flux gate ($\dot{b}$)	11.8
Front retreat (FR)	37.2
Frontal ablation (FA)	**43.7**
Total surface ablation ($SAbl$)	74.5
Total ablation (TA)	**118.2**

https://doi.org/10.5194/egusphere-2026-2298
Preprint. Discussion started: 6 May 2026
© Author(s) 2026. CC BY 4.0 License.

3.5. Broader implications

The study supports the growing body of evidence demonstrating that lake-terminating glaciers are governed by a complex suite of mechanical feedbacks that distinguish them from land-terminating systems (e.g., Benn et al., 2007b). The proposed model highlights how the hydraulic connection between the proglacial lake and the subglacial drainage system significantly reduces basal friction. For regions with glaciers in potential transition from land to lake-terminating, like Iceland (Aðalgeirsdóttir et al., 2020) and Greenland (Patton et al., 2016; Shugar et al., 2020), this implies that as proglacial lakes expand due to ongoing retreat in a warming climate, we can expect an acceleration in ice flow and enhanced mass loss as a result. The reduction in back-stress and the increase in basal water pressure, often approaching overburden pressure, facilitate hydro-fracturing and calving, creating a self-sustaining cycle of dynamic thinning and terminus recession (Sugiyama et al., 2011).

Specifically for the Icelandic context, such as the Vatnajökull Ice Cap margin, the findings suggest that the depth of proglacial lakes are primary drivers of glacier stability. As these lakes deepen as glaciers retreat in to overdeepened basins, the increased buoyancy will likely trigger more frequent and higher-magnitude calving events (Baurley et al., 2020; Benn et al., 2007b). This study provides an important framework for predicting the future evolution of Icelandic ice caps, where the rapid formation of new lakes is currently transforming almost stable land-terminating margins into highly sensitive lake-terminating ones, potentially leading to faster-than-predicted mass loss (Schomacker, 2010).

Both the observations and model demonstrate that frontal ablation plays an important role in total ablation at Skaftafellsjökull, highlighting the influence of the lake on glacier mass balance. Given the increasing number and area of proglacial lakes worldwide due to terminus retreat (Zhang et al., 2024a), these processes have the potential to become increasingly important to global glacier mass balance and thus sea level rise.

The implications for Greenland may be particularly significant given the extent of the ice-sheets land-terminating margin and since its peripheral glaciers are retreating and ice marginal lake area is increasing (Zhang et al., 2024a). Furthermore, bedrock over-deepenings are widespread beneath the ice sheets margins, especially where outlet systems follow deeply incised troughs (Patton et al., 2016), hence the transition to lake-terminating conditions in these systems could serve as a major catalyst for future accelerated discharge of inland ice. These considerations in conjunction with our study which underscores that the specific boundary conditions of proglacial lake-terminating glaciers critically impact their ice-dynamics and associated terminus mass loss, highlights the need to consider these systems in future projections of Greenland's contribution to global sea-level.

4. Conclusions

This study presents a computationally efficient modelling framework to analyse the transition of an Icelandic outlet glacier, Skaftafellsjökull, from a land- to a lake-terminating glacier. The model successfully reproduces the observed velocity patterns and captures the pronounced near-terminus acceleration between 2010 and 2018, reflecting the growing influence of the proglacial lake. The results indicate a threshold behaviour between effective pressure and ice velocity, whereby small decreases in effective pressure beyond a critical value result in strong accelerations, consistent with previous empirical observations (Iken and Bindschadler, 1986; Sugiyama et al., 2011). Furthermore, frontal ablation at the lake-terminating margin, accounted for roughly 37 % of total ablation between 2010 and 2018, highlighting the importance of the proglacial lake in accelerating mass loss via ice-dynamic processes.

Sensitivity experiments demonstrate that surface thinning exerts a much stronger control (3-4x greater) on near terminus velocity than terminus retreat. However, the influence of front retreat on terminus acceleration increases with time, and is expected to be greater in the future, as the glacier terminus retreats in to deeper water, in a similar process to that observed across large parts of West Antarctica where the bedrock of marine-terminating glaciers deepens inland resulting in grounding line retreat and ice sheet instability (e.g., Rignot et al., 2014).

Overall, our results provide further evidence highlighting the sensitivity of glacier dynamics to evolving proglacial lake conditions and the associated impact on near-terminus effective pressures. The modelling framework developed provides a

https://doi.org/10.5194/egusphere-2026-2298
Preprint. Discussion started: 6 May 2026
© Author(s) 2026. CC BY 4.0 License.

valuable tool for simulating these complex interactions in a computationally efficient manner. By capturing threshold behaviour in the effective pressure–velocity relationship, it contributes to an improved understanding of how lake-terminating glaciers will respond to ongoing climatic warming and the associated expansion of proglacial lakes. These insights could be essential for refining projections of future ice mass loss and its contribution to global sea-level rise.

Acknowledgements

We thank Eyjólfur Magnússon for providing a bedrock DEM of Öræfajökull Ice Cap. This work was supported by funding from the UK Natural Environment Research Council (NE/X01536X/1).

Author Contributions

JO, DG and PN designed the study. JO and YW processed the relevant data. JO developed the model and executed the experiments. JO also wrote the manuscript, with significant contribution from PN and DG. All authors contributed to and approved the final paper.

Competing interests

The authors declare no competing interests.

References

Aðalgeirsdóttir, G., Magnússon, E., Pálsson, F., Thorsteinsson, T., Belart, J. M. C., Jóhannesson, T., Hannesdóttir, H., Sigurðsson, O., Gunnarsson, A., Einarsson, B., Berthier, E., Schmidt, L. S., Haraldsson, H. H., and Björnsson, H.: Glacier changes in Iceland from ~1890 to 2019, Front. Earth Sci. (Lausanne)., 8, https://doi.org/10.3389/feart.2020.523646, 2020.

Baurley, N. R., Robson, B. A., and Hart, J. K.: Long-term impact of the proglacial lake Jökulsárlón on the flow velocity and stability of Breiðamerkurjökull glacier, Iceland, Earth Surf. Process. Landf., 45, 2647–2663, https://doi.org/10.1002/esp.4920, 2020.

Baurley, N. R., Andrews, A., Robson, B., Attia, S., Martinez, K., and Hart, J. K.: Contrasting Dynamic Behaviour of Five Lake-terminating Glaciers Draining the Vatnajökull Ice Cap and Links to Bedrock Topography, Remote Sens. Earth Syst. Sci., 8, 696–717, https://doi.org/10.1007/s41976-025-00213-8, 2025.

Benn, D. I., Hulton, N. R. J., and Mottram, R. H.: "Calving laws", "sliding laws" and the stability of tidewater glaciers, Ann. Glaciol., 46, 123–130, 2007a.

Benn, D. I., Warren, C. R., and Mottram, R. H.: Calving processes and the dynamics of calving glaciers, Earth. Sci. Rev., 82, 143–179, https://doi.org/10.1016/j.earscirev.2007.02.002, 2007b.

Bondzio, J. H., Seroussi, H., Morlighem, M., Kleiner, T., R??ckamp, M., Humbert, A., and Larour, E. Y.: Modelling calving front dynamics using a level-set method: Application to Jakobshavn Isbr??, West Greenland, Cryosphere, 10, 497–510, https://doi.org/10.5194/tc-10-497-2016, 2016.

Carrivick, J. L. and Tweed, F. S.: Proglacial Lakes: Character, behaviour and geological importance, Quat. Sci. Rev., 78, 34–52, https://doi.org/10.1016/j.quascirev.2013.07.028, 2013.

Carrivick, J. L., Tweed, F. S., Sutherland, J. L., and Mallalieu, J.: Toward Numerical Modeling of Interactions Between Ice-Marginal Proglacial Lakes and Glaciers, Front. Earth Sci. (Lausanne)., 8, https://doi.org/10.3389/feart.2020.577068, 2020.

https://doi.org/10.5194/egusphere-2026-2298
Preprint. Discussion started: 6 May 2026
© Author(s) 2026. CC BY 4.0 License.

Cook, S., Rutt, I. C., Murray, T., Luckman, A., Zwinger, T., Selmes, N., Goldsack, A., and James, T. D.: Modelling environmental influences on calving at Helheim Glacier in eastern Greenland, Cryosphere, 8, 827–841, https://doi.org/10.5194/tc-8-827-2014, 2014.

Cuffey, K. M. . and Paterson, W. S. B. .: The physics of glaciers, Elsevier/BH, 2010.

Dell, R., Carr, R., Phillips, E., and Russell, A. J.: Response of glacier flow and structure to proglacial lake development and climate at Fjallsjökull, south-east Iceland, Journal of Glaciology, 65, 321–336, https://doi.org/10.1017/jog.2019.18, 2019.

Foresta, L., Gourmelen, N., Pálsson, F., Nienow, P., Björnsson, H., and Shepherd, A.: Surface elevation change and mass balance of Icelandic ice caps derived from swath mode CryoSat-2 altimetry, Geophys. Res. Lett., 43, 12,138-12,145, https://doi.org/10.1002/2016GL071485, 2016.

Gagliardini, O., Cohen, D., Råback, P., and Zwinger, T.: Finite-element modeling of subglacial cavities and related friction law, J. Geophys. Res. Earth Surf., 112, 1–11, https://doi.org/10.1029/2006JF000576, 2007.

Gagliardini, O., Zwinger, T., Gillet-Chaulet, F., Durand, G., Favier, L., De Fleurian, B., Greve, R., Malinen, M., Martín, C., Räback, P., Ruokolainen, J., Sacchettini, M., Schäfer, M., Seddik, H., and Thies, J.: Capabilities and performance of Elmer/Ice, a new-generation ice sheet model, Geosci. Model Dev., 6, 1299–1318, https://doi.org/10.5194/gmd-6-1299-2013, 2013.

Geuzaine, C. and Remacle, J. F.: Gmsh: A 3-D finite element mesh generator with built-in pre- and post-processing facilities, Int. J. Numer. Methods Eng., 79, 1309–1331, https://doi.org/10.1002/nme.2579, 2009.

Gudmundsson, M. T., Thordarson, T., Hoskuldsson, A., Larsen, G., Bjornsson, H., Prata, F. J., Oddsson, B., Magnusson, E., Hognadottir, T., Petersen, G. N., Hayward, C. L., Stevenson, J. A., and Jonsdottir, I.: Ash generation and distribution from the April-May 2010 eruption of Eyjafjallajökull, Iceland, Sci. Rep., 2, https://doi.org/10.1038/srep00572, 2012.

Guðmundsson, S., Björnsson, H., Pálsson, F., Magnússon, E., Sæmundsson, Þ., and Jóhannesson, T.: Terminus lakes on the south side of Vatnajökull ice cap, SE-Iceland, Jokull, 2019, 1–34, https://doi.org/10.33799/jokull2019.69.001, 2019.

Hannesdóttir, H., Björnsson, H., Pálsson, F., Adalgeirsdóttir, G., and Gudmundsson, S.: Changes in the southeast Vatnajo7die;kull ice cap, Iceland, between ~1890 and 2010c, https://doi.org/10.5194/tc-9-565-2015, 19 March 2015.

Holt, E., Nienow, P., and Medina-Lopez, E.: Terminus thinning drives recent acceleration of a Greenlandic lake-terminating outlet glacier, Journal of Glaciology, 70, https://doi.org/10.1017/jog.2024.30, 2024.

Howat, I. M., Joughin, I., Tulaczyk, S., and Gogineni, S.: Rapid retreat and acceleration of Helheim Glacier, east Greenland, Geophys. Res. Lett., 32, 1–4, https://doi.org/10.1029/2005GL024737, 2005.

Iken, A. and Bindschadler, R. A.: Combined measurements of subglacial water pressure and surface velocity of Findelengletscher, Switzerland: conclusions about drainage system and sliding mechanism, Journal of Glaciology, 32, 101–119, 1986.

Jenkins, A.: Convection-driven melting near the grounding lines of ice shelves and tidewater glaciers, J. Phys. Oceanogr., 41, 2279–2294, https://doi.org/10.1175/JPO-D-11-03.1, 2011.

Jóhannesson, T., Björnsson, H., Magnússon, E., Gudmundsson, S., Pálsson, F., Sigurdsson, O., Thorsteinsson, T., and Berthier, E.: Ice-volume changes, bias estimation of mass-balance measurements and changes in subglacial lakes derived by lidar mapping of the surface of Icelandic glaciers, Ann. Glaciol., 54, 63–74, https://doi.org/10.3189/2013AoG63A422, 2013.

Jóhannesson, T., Pálmason, B., Hjartarson, Á., Jarosch, A. H., Magnússon, E., Belart, J. M. C., and Gudmundsson, M. T.: Non-surface mass balance of glaciers in Iceland, Journal of Glaciology, 66, 685–697, https://doi.org/10.1017/jog.2020.37, 2020.

Jouvet, G.: A multilayer ice-flow model generalising the shallow shelf approximation, J. Fluid Mech., 764, 26–51, https://doi.org/10.1017/jfm.2014.689, 2014.

King, O., Bhattacharya, A., Bhambri, R., and Bolch, T.: Glacial lakes exacerbate Himalayan glacier mass loss, Sci. Rep., 9, https://doi.org/10.1038/s41598-019-53733-x, 2019.

https://doi.org/10.5194/egusphere-2026-2298
Preprint. Discussion started: 6 May 2026
© Author(s) 2026. CC BY 4.0 License.

Lea, J. M.: The Google Earth Engine Digitisation Tool (GEEDiT) and the Margin change Quantification Tool (MaQiT) – Simple tools for the rapid mapping and quantification of changing Earth surface margins, Earth Surface Dynamics, 6, 551–561, https://doi.org/10.5194/esurf-6-551-2018, 2018.

Magnússon, E., Pálsson, F., Björnsson, H., and Guðmundsson, S.: Removing the ice cap of Öræfajökull central volcano, SE-Iceland: Mapping and interpretation of bedrock topography, ice volumes, subglacial troughs and implications for hazards assessments, Jökull, 62, 131–150, https://doi.org/10.33799/jokull2012.62.131, 2012.

Magnússon, E., Pálsson, F., Björnsson, H., and Guðmundsson, S.: Erratum in; Removing the ice cap of Öraefajökull central volcano, SE-Iceland: Mapping and interpretation of bedrock topography, ice volumes, subglacial troughs and implications for hazards assessments, Jökull, 64, 83–84, https://doi.org/10.33799/jokull2014.64.083o, 2014.

McNabb, R. W. and Hock, R.: Alaska tidewater glacier terminus positions, 1948-2012, J. Geophys. Res. Earth Surf., 119, 153–167, https://doi.org/10.1002/2013JF002915, 2014.

McNabb, R. W., Hock, R., and Huss, M.: Variations in Alaska tidewater glacier frontal ablation, 1985-2013, J. Geophys. Res. Earth Surf., 120, 120–136, https://doi.org/10.1002/2014JF003276, 2015.

Minowa, M., Schaefer, M., Sugiyama, S., Sakakibara, D., and Skvarca, P.: Frontal ablation and mass loss of the Patagonian icefields, Earth Planet. Sci. Lett., 561, 116811, https://doi.org/10.5281/zenodo.3899570, 2021.

Moon, T. and Joughin, I.: Changes in ice front position on Greenland's outlet glaciers from 1992 to 2007, J. Geophys. Res. Earth Surf., 113, https://doi.org/10.1029/2007JF000927, 2008.

Noël, B., Aðalgeirsdóttir, G., Pálsson, F., Wouters, B., Lhermitte, S., Haacker, J. M., and van den Broeke, M. R.: North Atlantic Cooling is Slowing Down Mass Loss of Icelandic Glaciers, Geophys. Res. Lett., 49, https://doi.org/10.1029/2021GL095697, 2022.

Nuth, C. and Kääb: Co-registration and bias corrections of satellite elevation data sets for quantifying glacier thickness change, Cryosphere, 5, 271–290, https://doi.org/10.5194/tc-5-271-2011, 2011.

Patton, H., Swift, D. A., Clark, C. D., Livingstone, S. J., and Cook, S. J.: Distribution and characteristics of overdeepenings beneath the Greenland and Antarctic ice sheets: Implications for overdeepening origin and evolution, Quat. Sci. Rev., 148, 128–145, https://doi.org/10.1016/j.quascirev.2016.07.012, 2016.

Pfeffer, W. T.: A simple mechanism for irreversible tidewater glacier retreat, J. Geophys. Res. Earth Surf., 112, https://doi.org/10.1029/2006JF000590, 2007.

Porter, C., Morin, P., Howat, I., Noh, M.-J., Bates, B., Peterman, K., Keesey, S., Schlenk, M., Gardiner, J., Tomko, K., Willis, M., Kelleher, C., Cloutier, M., Husby, E., Foga, S., Nakamura, H., Platson, M., Wethington Michael, Jr., Williamson, C., Bauer, G., Enos, J., Arnold, G., Kramer, W., Becker, P., Doshi, A., D'Souza, C., Cummens, P., Laurier, F., and Bojesen, M.: ArcticDEM, Version 3, https://doi.org/10.7910/DVN/OHHUKH, 2018.

Porter, C., Howat, I., Noh, M.-J., Husby, E., Khuvis, S., Danish, E., Tomko, K., Gardiner, J., Negrete, A., Yadav, B., Klassen, J., Kelleher, C., Cloutier, M., Bakker, J., Enos, J., Arnold, G., Bauer, G., and Morin, P.: ArcticDEM - Strips, Version 4.1, https://doi.org/10.7910/DVN/C98DVS, 2022.

Pronk, J. B., Bolch, T., King, O., Wouters, B., and Benn, D. I.: Contrasting surface velocities between lake-and land-terminating glaciers in the Himalayan region, Cryosphere, 15, 5577–5599, https://doi.org/10.5194/tc-15-5577-2021, 2021.

RGI Consortium: Randolph Glacier Inventory - A Dataset of Global Glacier Outlines, Version 6, Boulder, Colorado, USA, https://doi.org/https://doi.org/10.7265/4m1f-gd79, 2017.

Rignot, E., Mouginot, J., Morlighem, M., Seroussi, H., and Scheuchl, B.: Widespread, rapid grounding line retreat of Pine Island, Thwaites, Smith, and Kohler glaciers, West Antarctica, from 1992 to 2011, Geophys. Res. Lett., 41, 3502–3509, https://doi.org/10.1002/2014GL060140, 2014.

https://doi.org/10.5194/egusphere-2026-2298
Preprint. Discussion started: 6 May 2026
© Author(s) 2026. CC BY 4.0 License.

Robinson, A., Goldberg, D., and Lipscomb, W. H.: A comparison of the stability and performance of depth-integrated ice-dynamics solvers, Cryosphere, 16, 689–709, https://doi.org/10.5194/tc-16-689-2022, 2022.

Röhl, K.: Thermo-erosional notch development at fresh-water-calving Tasman Glacier, New Zealand, Journal of Glaciology, 52, 203–213, https://doi.org/10.3189/172756506781828773, 2006.

Schomacker, A.: Expansion of ice-marginal lakes at the Vatnajökull ice cap, Iceland, from 1999 to 2009, Geomorphology, 119, 232–236, https://doi.org/10.1016/j.geomorph.2010.03.022, 2010.

Schoof, C.: The effect of cavitation on glacier sliding, Proceedings of the Royal Society A: Mathematical, Physical and Engineering Sciences, 461, 609–627, https://doi.org/10.1098/rspa.2004.1350, 2005.

Shepherd, A., Ivins, E., Rignot, E., Smith, B., van den Broeke, M., Velicogna, I., Whitehouse, P., Briggs, K., Joughin, I., Krinner, G., Nowicki, S., Payne, T., Scambos, T., Schlegel, N., A, G., Agosta, C., Ahlstrøm, A., Babonis, G., Barletta, V. R., Bjørk, A. A., Blazquez, A., Bonin, J., Colgan, W., Csatho, B., Cullather, R., Engdahl, M. E., Felikson, D., Fettweis, X., Forsberg, R., Hogg, A. E., Gallee, H., Gardner, A., Gilbert, L., Gourmelen, N., Groh, A., Gunter, B., Hanna, E., Harig, C., Helm, V., Horvath, A., Horwath, M., Khan, S., Kjeldsen, K. K., Konrad, H., Langen, P. L., Lecavalier, B., Loomis, B., Luthcke, S., McMillan, M., Melini, D., Mernild, S., Mohajerani, Y., Moore, P., Mottram, R., Mouginot, J., Moyano, G., Muir, A., Nagler, T., Nield, G., Nilsson, J., Noël, B., Otosaka, I., Pattle, M. E., Peltier, W. R., Pie, N., Rietbroek, R., Rott, H., Sandberg Sørensen, L., Sasgen, I., Save, H., Scheuchl, B., Schrama, E., Schröder, L., Seo, K. W., Simonsen, S. B., Slater, T., Spada, G., Sutterley, T., Talpe, M., Tarasov, L., van de Berg, W. J., van der Wal, W., van Wessem, M., Vishwakarma, B. D., Wiese, D., Wilton, D., Wagner, T., Wouters, B., and Wuite, J.: Mass balance of the Greenland Ice Sheet from 1992 to 2018, Nature, 579, https://doi.org/10.1038/s41586-019-1855-2, 2020.

Shugar, D. H., Burr, A., Haritashya, U. K., Kargel, J. S., Watson, C. S., Kennedy, M. C., Bevington, A. R., Betts, R. A., Harrison, S., and Strattman, K.: Rapid worldwide growth of glacial lakes since 1990, Nat. Clim. Chang., 10, 939–945, https://doi.org/10.1038/s41558-020-0855-4, 2020.

Sugiyama, S., Skvarca, P., Naito, N., Enomoto, H., Tsutaki, S., Tone, K., Marinsek, S., and Aniya, M.: Ice speed of a calving glacier modulated by small fluctuations in basal water pressure, Nat. Geosci., 4, 597–600, https://doi.org/10.1038/ngeo1218, 2011.

Sutherland, J. L., Carrivick, J. L., Gandy, N., Shulmeister, J., Quincey, D. J., and Cornford, S. L.: Proglacial Lakes Control Glacier Geometry and Behavior During Recession, Geophys. Res. Lett., 47, https://doi.org/10.1029/2020GL088865, 2020.

Thomas, R. H.: Force-perturbation analysis of recent thinning and acceleration of Jakobshavn Isbræ, Greenland, Journal of Glaciology, 50, 57–66, https://doi.org/10.3189/172756504781830321, 2004.

Truffer, M. and Motyka, R. J.: Where glaciers meet water: Subaqueous melt and its relevance to glaciers in various settings, https://doi.org/10.1002/2015RG000494, 1 March 2016.

Trüssel, B. L., Motyka, R. J., Truffer, M., and Larsen, C. F.: Rapid thinning of lake-calving Yakutat Glacier and the collapse of the Yakutat Icefield, southeast Alaska, USA, Journal of Glaciology, 59, 149–161, https://doi.org/10.3189/2013J0G12J081, 2013.

Tsutaki, S., Nishimura, D., Yoshizawa, T., and Sugiyama, S.: Changes in glacier dynamics under the influence of proglacial lake formation in Rhonegletscher, Switzerland, Ann. Glaciol., 52, 31–36, https://doi.org/10.3189/172756411797252194, 2011.

Tsutaki, S., Fujita, K., Nuimura, T., Sakai, A., Sugiyama, S., Komori, J., and Tshering, P.: Contrasting thinning patterns between lake- And land-terminating glaciers in the Bhutanese Himalaya, Cryosphere, 13, 2733–2750, https://doi.org/10.5194/tc-13-2733-2019, 2019.

Van Der Veen, C. J.: Fracture mechanics approach to penetration of surface crevasses on glaciers, Cold Reg. Sci. Technol., 27, 31–47, https://doi.org/10.1016/S0165-232X(97)00022-0, 1998.

Weis, M., Greve, R., and Hutter, K.: Theory of shallow ice shelves, Continuum Mech. Thermodyn, Springer-Verlag, 15–50 pp., 1999.

https://doi.org/10.5194/egusphere-2026-2298
Preprint. Discussion started: 6 May 2026
© Author(s) 2026. CC BY 4.0 License.



595 Wu, K., Bolch, T., Cheng, P., Baldacchino, F., Duan, Y., Ma, D., and Liu, S.: Assessing the dynamic changes and the effect of buoyancy of lake-terminating Yanong Glacier in the southeastern Tibetan Plateau with UAV surveys, J. Hydrol. Reg. Stud., 59, https://doi.org/10.1016/j.ejrh.2025.102385, 2025.

xDEM contributors: xDEM (v0.1.0), https://doi.org/10.5281/zenodo.11492983, 2024.

Zhang, G., Carrivick, J. L., Emmer, A., Shugar, D. H., Veh, G., Wang, X., Labedz, C., Mergili, M., Mölg, N., Huss, M., Allen, S.,
600 Sugiyama, S., and Lützow, N.: Characteristics and changes of glacial lakes and outburst floods, https://doi.org/10.1038/s43017-024-00554-w, 1 June 2024a.

Zhang, T., Wang, W., and An, B.: Heterogeneous changes in global glacial lakes under coupled climate warming and glacier thinning, Commun. Earth Environ., 5, https://doi.org/10.1038/s43247-024-01544-y, 2024b.